# Semiautomatic Segmentation of Rim Area Focal Hyperautofluorescence Predicts Progression of Geographic Atrophy Due to Dry Age-Related Macular Degeneration

Michael J. Allingham,[1] Qing Nie,[2] Eleonora M. Lad,[1] Daniel J. Izatt,[3] Priyatham S. Mettu,[1] Scott W. Cousins,[1] and Sina Farsiu[4]

[1]Department of Ophthalmology, Duke University Medical Center, Durham, North Carolina, United States
[2]Beijing Institute of Technology, Beijing, China
[3]Enloe High School, Raleigh, North Carolina, United States
[4]Department of Ophthalmology, Duke University Medical Center, Durham, North Carolina, United States, Department of Biomedical Engineering, Duke University, Durham, North Carolina, United States

Correspondence: Michael J. Allingham, DUMC Box 3802, Durham, NC 27710, USA; mike.allingham@dm.duke.edu.

Submitted: December 22, 2015
Accepted: March 18, 2016

Citation: Allingham MJ, Nie Q, Lad WM, et al. Semiautomatic segmentation of rim area focal hyperautofluorescence predicts progression of geographic atrophy due to dry age-related macular degeneration. *Invest Ophthalmol Vis Sci*. 2016;57:2283–2289. DOI:10.1167/iovs.15-19008

**Purpose.** To develop image analysis software usable by nonexpert graders to segment geographic atrophy (GA) from dry AMD and to quantify rim area focal hyperautofluorescence (RAFH) surrounding GA on fundus autofluorescence (FAF) images. To compare the GA progression predictions based on RAFH with those of a validated qualitative classification system.

**Methods.** Retrospective analysis of serial FAF images from 49 eyes of 30 subjects with GA was performed using MATLAB-based software (MathWorks, Natick, MA, USA). Correlation between RAFH and progression of GA was analyzed using Spearman correlation. Comparisons of lesion growth rate between RAFH tertiles used generalized estimating equations and Kruskal-Wallis testing. Interobserver variability in lesion size, growth rate and RAFH were compared between two expert and one nonexpert grader using Bland-Altman statistics.

**Results.** Rim area focal hyperautofluorescence was positively correlated with GA progression rate ($\rho = 0.49$, $P < 0.001$). Subjects in the middle or highest RAFH tertile were at greater risk of progression ($P = 0.005$ and $P = 0.001$, respectively). Mean difference in RAFH was 0.012 between expert and −0.005 to 0.017 between expert and nonexperts. Mean difference in lesion size ($mm^2$) was 0.11 between expert and −0.29 to 0.41 between expert and nonexperts. Mean difference in lesion growth rate ($mm^2$/mo) was 0.0098 between expert and −0.027 to 0.037 between expert and nonexperts. Risk stratification based on RAFH tertile was 96% identical across all graders.

**Conclusions.** Our semiautomated image analysis software facilitates stratification of progression risk based on RAFH and enabled a nonexpert grader with minimal training to obtain results comparable to expert graders. Predictions based on RAFH were similar to those of a validated qualitative classification system.

Keywords: geographic atrophy, fundus autofluorescence, image analysis

Geographic atrophy (GA) is a visually disabling form of dry AMD[1] and is responsible for 20% of late stage AMD in the United States.[1] Clinically, GA manifests as loss of the retinal pigment epithelium (RPE), overlying retina and underlying choriocapillaris.[2] Currently, there is no Food and Drug Administration–approved therapy for patients afflicted with GA. While several clinical trials have been undertaken and others are ongoing, one of the main obstacles faced by investigators is the long follow-up required to detect therapeutic efficacy. Thus, the ability to accurately and easily predict patients at risk for GA progression would be beneficial for future clinical studies and may also identify appropriate candidates for treatment when treatment becomes available.

Recent studies using structural ophthalmic imaging technologies (e.g., spectral-domain optical coherence tomography [SD-OCT]), while providing excellent results in visualizing the biomarkers of the current stage of dry AMD, have shown promising but far from ideal performance in predicating GA progression.[3–7] Functional imaging systems may provide complementary information about cells that have not yet structurally deteriorated. For example, fundus autofluorescence (FAF) is a noninvasive ocular imaging technique, which detects endogenous fluorophores present in the retina. Fundus autofluorescence imaging is frequently used to monitor GA clinically and has been successfully used to quantify the size of GA lesions.[8–13]

Lipofuscin granules in the RPE are hypothesized to be the primary source of autofluorescence in retina.[14,15] There are multiple proposed mechanisms of hyperautofluorescence at GA lesion borders.[16,17] Moreover, there are differing reports as to whether hyperautofluorescence is predictive of lesion progression. The majority of previous studies have demonstrated that either the pattern or intensity of hyperautofluorescence at the edges of GA lesions is predictive of GA progression[10,18,19] (Bearelly S, et al. *IOVS* 2010;51:E-Abstract 531). However, others have not found a correlation between border zone

hyperautofluorescence and GA progression.[20] Holz and colleagues[10] have generated a classification system that associates specific patterns of FAF with age of onset and risk of progression.[21–23] However, this classification system requires a trained analyst and may not be reproducible between different observers.[24] Seeking a simpler means of predicting GA progression, Bearelly and colleagues[25] performed a retrospective analysis of autofluorescence in which the rim area, defined as the 500 μm surrounding GA lesions, was qualitatively categorized according to its level of hyperautofluorescence. In this cohort, the rate of GA progression was faster in subjects with the most rim area focal hyperautofluorescence (RAFH) compared with those with the lowest RAFH. By contrast, Hwang et al.[20] used semiautomated segmentation of GA and lesion border hyperautofluorescence and found no significant relationship between areas of hyperautofluorescence and areas of GA progression.

The goals of the current study were (1) to generate and validate algorithms and user friendly software capable of segmenting GA area and RAFH even when used by nonexpert graders, and (2) to determine whether quantification of RAFH could predict risk of GA progression with similar accuracy compared with the prospectively validated qualitative classification system of Holz.

## Methods

### Subjects

This study was approved by the Duke University Medical Center institutional review board (Durham, NC, USA), was conducted in compliance with the Health Insurance Portability and Accountability Act (HIPAA) and adhered to the tenets of the Declaration of Helsinki. Subjects with GA secondary to dry AMD who received FAF imaging as part of their routine care between 1/1/2005 and 12/31/10 were identified. Subjects with a history of neovascular AMD, myopia greater than 6 diopters (D), or other macular pathology were excluded. Subjects were required to have total GA area exceeding 1 $mm^2$ at baseline and to have undergone FAF imaging at least 6 months apart.

Based on these criteria, 43 subjects were identified and their FAF images were obtained for analysis. Image quality was graded based on the definition of vascular structures and classified as good, fair, or poor. Images that were of poor quality or in which the GA lesion extended beyond the edge of the image were excluded from analysis. Images for one subject could not be located. Ultimately, 49 eyes from 30 subjects were included in the study.

### Image Acquisition

All images for this study were obtained using the Heidelberg Retina Angiograph 2 (HRA2; Heidelberg, Germany) device and the standard 30° field of view (768 × 768 pixels) as previously described.[25] Briefly, the standard image acquisition protocol used excitation at 488 nm via an optically pumped solid state laser and a barrier filter set for detection above 500 nm. Nine to 15 images were averaged to form a mean image. All images were obtained using the Automatic Real Time (ART) mode.

### Image Analysis

For each eye, two FAF images obtained at least 6 months apart were analyzed. Representative samples of images and image analysis are shown in Figure 1. For each image, the vessels and optic nerve head (ONH) were first segmented out. Vessels were automatically detected using Dijkstra forest based automatic vessel segmentation[26] and then removed using in-paint technology using a traditional in-painting method by solving Laplace's equation.[4] Next, the ONH was automatically identified by taking advantage of the fact that it is a round hypoautofluorescent region located at the border of the image. Specifically, the algorithm first obtained the average intensity of the image by filtering the image with a disk averaging filter. The radius of the disk filter is 80 pixels, which corresponds to the approximate size of the ONH. After disk filtering, the areas comprising the lowest 5% average intensity were taken as candidate ONH regions. Finally, the largest of these low-intensity regions located at the border of the image was selected as the ONH region. The mean intensity of the ONH region was termed $M_{onh}$.

Next, we segmented the GA area, which corresponds to hyperautofluorescent regions. Simple thresholding cannot be used for segmentation as FAF images often have uneven illumination. This artifact is due to an optical aberration called vignetting or due to the optics system used to capture the images and can hinder direct interpretation of the pixel intensity information.

We detected GA by using both an absolute pixel intensity threshold and by considering local variation in pixel intensity. In detail, after obtaining the mean intensity of the ONH, $M_{onh}$, we first generated a binary image $I_{bw1}$ by using $M_{onh}$ as reference threshold. Areas where pixel intensity fell below this threshold were considered candidate GA regions. A second binary image, $I_{bw2}$, was generated using a local pixel intensity comparison as below:

$$I_{bw2}(r,c) = \Big(X(r,c) - M(r,c)\Big) < \text{threshold} \qquad (1)$$

Here $X(r,c)$ represents the FAF intensity value (ranging from 0–255) in position $(r,c)$. $M(r,c)$ represents the mean intensity value within a $400 \times 400$ pixel window centered at $(r,c)$. Many factors including settings during image acquisition, media opacity, eye movements, and subject positioning cause variation in FAF intensity between images. To compensate for these variations between images, our software provides a slider allowing manual adjustment of the threshold parameter by the grader.

When both binary images ($I_{bw1}$ and $I_{bw2}$) had been generated, we calculated their union as a pilot candidate GA region estimate. We next employed a series of modified morphologic close operations to fill the holes in the region, combine neighboring regions, and smooth the region border. To achieve this, we first eroded the image using a disk structuring element with a radius of 10. Then, we dilated the image using a disk structuring element with a radius of 12, followed by eroding the image again using a disk structuring element with a radius of 12. Finally, we removed small regions spanning less than 3000 pixels. The remaining region is the candidate GA region.

Segmentation of GA in some cases required manual adjustment especially when GA is contiguous with peripapillary atrophy and cases of normal foveal hypoautofluorescence. Accordingly, the software contains tools that allow the grader to manually segment portions of the image, a slider to adjust the threshold of GA detection at the automatically determined lesion borders and a custom region selector that permits local pixel intensity analysis of a user selected region.

After the GA border had been defined, the software automatically generated a second line 40 pixels (approximately 440 μm) beyond the GA border. We defined the space between this line and the GA border as the rim area. A rim area of 440 μm was selected based on two factors: the prior observation by Bearelly et al.[25] that increased RAFH within approximately 500 μm of the GA lesion border was associated with increased rate of lesion growth, and based on the observation in FAF images not part of the study that nearly all RAFH was contained within

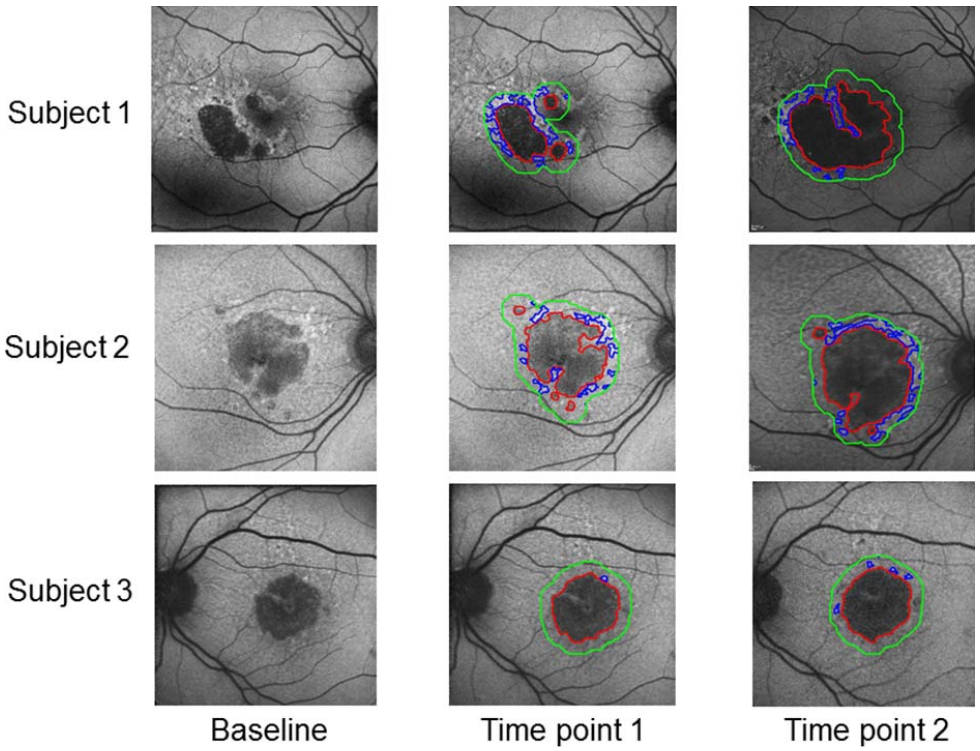


**Figure 1.** Representative baseline images and output from the semiautomated software analysis algorithm from subjects of each RAFH tertile. Baseline photos are shown on the *left*. Geographic atrophy is outlined in *red* and the outer border of the rim area is outlined in *green*. Rim area hyperautofluorescence is outlined in *blue*. Subject one and two had high and medium RAFH, respectively, and significant progression in lesion size. Subject three had low RAFH and minimal lesion growth.

450 μm of the lesion borders. A second local intensity comparison using a threshold of +50 pixels is performed to identify the hyperautofluorescent pixels within the rim area. Rim area focal hyperautofluorescence was automatically calculated as the ratio of hyperautofluorescent rim area to total rim area.

### Image Segmentation by Human Graders

Images were segmented by three graders; two retina clinicians (MA and EL) and one nonclinician high school student (DI). All graders were familiarized with the use of the software and allowed to practice on FAF images, which were not part of this study prior to grading. In addition, the nonclinician grader was given a 2-hour lecture regarding GA, the technical aspects of FAF, normal, and pathologic findings on FAF, particularly those present in patients with AMD and GA. Graders were instructed to adjust the automatic GA lesion segmentation if needed by first adjusting the sensitivity threshold for detecting GA using a slider in the software. Next small areas of GA, which were left unsegmented could be incorporated using a selection tool allowing automatic local pixel analysis of a user selected region. Finally, in cases where foveal hypoautofluorescence was segmented as GA or when GA was contiguous with the optic nerve, manual segmentation was allowed. Following this training, all graders segmented each image independently using the same computer under identical lighting conditions.

### Statistical Analysis

Correlation between RAFH at study entry and GA progression measured in millimeters squared ($mm^2$) per month was analyzed using Spearman correlation. Median lesion size or GA growth rate among RAFH tertiles were compared using Kruskal-Wallis testing after accounting for correlation between eyes from the same individual using generalized estimating equations. Intraobserver variability was quantified using Bland-Altman statistics. Statistical analysis was performed using SAS software (SAS Institute, Cary, NC, USA). Statistical significance was defined as $P < 0.05$.

## Results

Among the 30 subjects included in the study, the average age was 79.1. Twenty subjects were female and 10 were male. All subjects except one were self-identified as Caucasian; the non-Caucasian patient did not have their race recorded in the medical record. The mean time between acquisition of the first and second FAF images was 15.6 months (median, 13 months; interquartile range [IQR], 8–21; range, 6–32 months). Mean lesion size at the first time-point was 7.55 $mm^2$ (median, 6.25 $mm^2$). Thirty eyes had unifocal lesions and 19 had multifocal lesions. In eyes with multifocal lesions, the mean number of lesions was four and maximum was eight. The mean growth rate was 0.16 $mm^2$/mo and 1.92 $mm^2$/y (median, 1.68 $mm^2$/y).

Bearelly et al.[25] have previously demonstrated that GA lesions subjectively graded as having high RAFH by expert graders have a higher rate of GA progression. To confirm this finding, we examined the correlation between RAFH and the rate of GA lesion growth and found a positive correlation between RAFH and rate of GA lesion growth (Spearman correlation coefficient 0.49, $P < 0.001$). A scatterplot of GA lesion growth rate versus RAFH at the first time-point is shown in Figure 2. Eyes were next separated into tertiles by RAFH and the median lesion size and growth rate were compared (Table 1).

The difference between the lowest RAFH tertile and the middle and upper RAFH tertiles were statistically significant (*P*

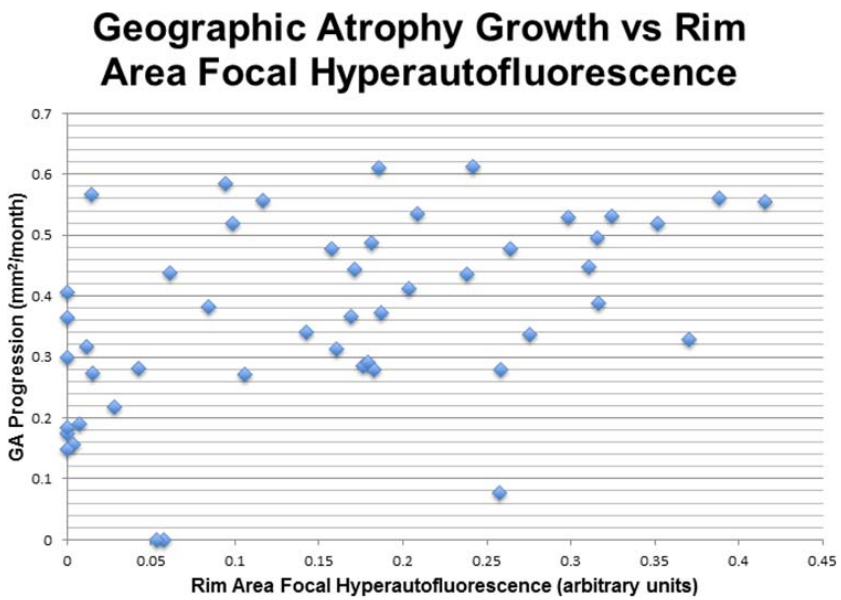


**Figure 2.** Graph of GA progression versus RAFH. Spearman correlation coefficient was 0.49 ($P < 0.001$).

$= 0.005$ for medium versus low and $P = 0.001$ for high versus low). Global comparison of tertiles was also statistically significant ($P = 0.001$).

In order to determine reproducibility of our algorithm and whether our software could be used by nonexpert graders, two expert retina clinician graders, and one nonclinician nonexpert grader used the software to segment GA and RAFH in all study eyes. All graders reported being able to use the software without difficulty and took under 1 minute to segment each image on average. All three graders made some adjustment in the automatic GA segmentation of most eyes (range, 80–88 of 98 total images). Most adjustments were minor alterations to the GA lesion border and only 13 images required use of the hand drawing tool due to foveal hypoautofluorescence or GA contiguous with the optic nerve. To compare the results of segmentation performed by expert and nonexpert graders, we used Bland-Altman analysis (Table 2). Mean difference in RAFH was 0.012 between expert graders and –0.005 to 0.017 between expert and nonexpert graders. Mean difference in lesion size was 0.11 $mm^2$ between expert graders and –0.29 to 0.41 $mm^2$ between expert and nonexpert graders. Mean difference in lesion growth rate was 0.0098 $mm^2$/mo between expert graders and –0.027 to 0.037 $mm^2$/mo between expert and nonexpert graders.

Mean agreements for interobserver variability for lesion size are similar to previously reported values using commercial software for GA segmentation using trained graders in a reading center.[12] Agreement between graders for lesion progression was somewhat less than those of Schmitz-Valckenberg et al.[12] when comparing expert and nonexpert graders. Importantly, mean agreement between all graders for RAFH was extremely high, which resulted in risk stratification based on RAFH tertile being 96% identical across all three graders. Specifically, there was complete agreement between the nonexpert grader and one expert and there was discrepancy in only 2 of 49 eyes when comparing the nonexpert grader and the other expert. This demonstrates that, following minimal training, a nonexpert can easily learn to operate the software and can generate predictions comparable with an expert.

Finally, we compared the predictions of our software with those based on patterns of FAF described by Holz and colleagues.[10,21] Two expert retina clinicians (PM and SC) were masked to the output of our software and were asked to classify by consensus the FAF pattern present in the first image of each eye using the stock images and algorithm published by Holz and colleagues.[10,21] Results of this analysis are shown in Table 3.

In our cohort, eight eyes had low risk patterns of FAF ("none" or "focal"). Of these, seven were in the lowest RAFH tertile and five fell into the lowest decile of RAFH. This suggests that our software with the Holz algorithm in identifying eyes at low risk of progression. Holz and colleagues[10] have delineated six patterns of FAF which are associated with increased GA progression; "banded," and five subtypes of "diffuse" pattern FAF. In our cohort, eight of nine eyes displaying a "banded" FAF pattern were in the highest RAFH tertile. Thirty-two eyes displayed a "diffuse" pattern of FAF. Of these, 71.9% were in the middle or upper RAFH tertiles. These results suggest that our software correctly identifies eyes likely to experience rapid GA progression and that eyes with very low RAFH are at low risk of progression.

## Discussion

The purpose of this study was to develop a rapid, objective means of quantifying GA and RAFH that is usable by nonexpert graders and to demonstrate that predictions based on quantification of RAFH are comparable to those of the current gold standard qualitative classification system. The current study is unique in its inclusion of a nonexpert grader. When compared with our two expert graders, the nonexpert grader

**Table 1.** GA Growth Rate by Tertile of Rim Area Focal Hyperautofluorescence

| RAFH Tertile | Median GA Growth Rate ($mm^2$/mo) |
|---|---|
| Low | 0.08 (0.03–0.14) |
| Middle | 0.15 (0.08–0.26)* |
| High | 0.24 (0.12–0.28)† |

* $P = 0.005$ for low vs. middle.

† $P = 0.001$ for low vs. high. Data is reported as median (25th–75th percentile).

**Table 2.** Mean Differences and 95% Confidence Intervals for Interobserver Agreements for Initial Lesion Size, Lesion Growth Rate, and RAFH

| Readers | Initial Lesion Size (mm²) | GA Growth Rate (mm²/mo) | RAFH |
|---|---|---|---|
| Expert 1–Expert 2 | 0.12 (±0.23) | 0.12 (±0.37) | 0.012 (±0.006) |
| Expert 1–Nonexpert | −0.29 (±0.41) | 0.44 (±0.79) | −0.005 (±0.006) |
| Expert 2–Nonexpert | 0.41 (±0.47) | −0.33 (±0.84) | 0.017 (±0.008) |

Mean agreement between graders was assessed using Bland-Altman statistics. Mean agreement (±95% confidence interval) for initial lesion size, GA growth rate, and RAFH are shown for all grader combinations.

was able to use the software to generate nearly identical RAFH-based predictions of GA progression. Importantly, the predictions of our software correlate well with those based on the Holz FAF pattern system. While RAFH does correlate with GA progression, this technology does not completely replace the qualitative categorization algorithms, which have been previously validated. There are certain diffuse FAF patterns such as "branching" and "fine granular," which are less well segmented by our software. Our findings are complementary to those of Holz and support the concept that hyperautofluorescence at GA lesion borders is correlated with GA progression and that FAF may be a marker of RPE dysfunction in GA. Our software could serve as a GA risk prediction algorithm that is useful when it is impractical to have images evaluated by expert graders in a reading center.

Analysis of images from our study cohort demonstrates a statistically significant, positive correlation between RAFH and rate of GA lesion growth. Study subjects in the top or middle tertile of RAFH had a significantly greater rate of GA growth when compared with those in the bottom tertile. This is in agreement with previous studies which have demonstrated a positive correlation between hyperautofluorescence at the borders of GA lesions and growth of GA.[9,25] In contrast to our findings, Hwang et al.[20] reported that total area of hyperautofluorescence in the rim area surrounding GA fails to predict progression. This disparity may be explained by several factors. First, the study cohort used by Hwang et al.[20] included only eight eyes of six subjects raising the possibility that our larger cohort was capable of identifying correlations not detectable in smaller groups. Second, the algorithm used by Hwang et al.[20] uses a single threshold across the entire image to define RAFH, whereas ours uses a combination of a global threshold and a local area intensity measurement to compensate for variations in autofluorescence intensity across individual images. Thus, RAFH as defined by our algorithm differs substantially from previously published work and may therefore have superior predictive value.

Certain GA lesion characteristics have been associated with increased rate of progression. For instance, GA has been shown to grow more rapidly along its peripheral borders compared with those adjacent to the fovea[27] and lesions, which are extrafoveal grow more rapidly than those already involving the fovea.[28] Additionally, multifocal GA has been found to progress more rapidly than unifocal GA.[6,28–30] In our cohort, the growth rate in multifocal and unifocal lesions was 0.14 (IQR, 0.08–0.28) and 0.14 (IQR, 0.08–0.25), respectively ($P = 0.89$). The median growth rate in foveal and extrafoveal lesions was 0.11 (IQR, 0.07–0.24) and 0.15 (IQR, 0.08–0.28), respectively ($P = 0.74$). The reason for the discrepancy between our study and previously published work is not immediately apparent. However, it may be that due to its relatively small size our study was not powered to detect these differences.

While FAF has long been used as a means to quantify GA and predict progression, numerous recent studies have used morphologic findings from SD-OCT to predict the rate or location of GA lesion growth. Several markers have been variably associated with GA progression including outer retinal tubulations (ORT),[6] ellipsoid zone disruption at GA borders,[3,4] alterations in reflectivity of the outer nuclear layer,[7] and various alterations in the RPE/Bruch's membrane complex.[5,6] Outer retinal tubulations have been associated with numerous retinal pathologies including GA.[31] In a study of 43 eyes with GA, Moussa et al.[6] identified ORT within the atrophic zone, but not at the GA border as a risk factor for GA progression. However, Hariri et al.[32] found that in a study of 108 eyes presence of ORT was associated with slower progression of GA. Thus, the predictive value of ORT remains unclear. Ellipsoid zone (EZ) loss at the GA border region was initially described by Bearelly et al.[33] who performed analysis of SD-OCT B-scans to characterize the morphology of GA lesion

**Table 3.** Classification of Study Subjects by Holz Qualitative Analysis of Fundus Autofluorescence Patterns

| | RAFH Tertile | | | |
|---|---|---|---|---|
| FAF Pattern | Low | Middle | High | Total |
| None | 6 (100) | | | 6 |
| Focal | 1 (50) | 1 (50) | | 2 |
| Banded | | 1 (11.1) | 8 (88.9) | 9 |
| Patchy | | | | 0 |
| Reticular | | 3 (60) | 2 (40) | 5 |
| Branching | 4 (80) | 1 (20) | | 5 |
| Fine granular | 2 (18.2) | 7 (63.6) | 2 (18.2) | 11 |
| Fine granular with peripheral punctate spots | 3 (42.8) | 2 (28.6) | 2 (28.6) | 7 |
| Trickling | | 2 (50) | 2 (50) | 4 |
| All diffuse | 9 (28.1) | 15 (46.9) | 8 (25) | 32 |

The initial FAF image for each study eye was classified according to the Holz FAF pattern system previously described.[10,21] The classification of eyes in each RAFH tertile are displayed in columns labeled low, middle, and high. The dashed line divides patterns of "low risk of progression" above and those considered "high risk of progression" below. The row labeled "All diffuse" represents the sum of all 5 diffuse FAF subtypes. Data are displayed as absolute number (percent of total eyes with that FAF pattern).

Investigative Ophthalmology & Visual Science

borders. More recently, en face analysis of SD-OCT has been used to quantify EZ loss as a potential particularly those without reticular pseudodrusen, it was not a robust predictor in a real world cohort.[3] Interestingly however, Nunes et al.[4] found that in select cases, EZ loss very accurately predicts the specific location of future GA within 12 months. While this methodology holds promise, its use is limited because it is unknown whether areas with EZ loss are irreversibly destined to become atrophic and if so over what time period atrophy will develop. Intriguingly, Stetson and colleagues[7] found that increased reflectivity of the outer nuclear layer or Henle fiber layer (ONL/HFL), which manifests as higher minimum pixel intensity along individual A-scans between the inner limiting membrane and RPE is correlated with rate of GA progression. They speculate that this change in the ONH/HFL may be due to early degenerative changes in the photoreceptors that precede development of GA. Finally, several different abnormalities of the RPE and subRPE space have been associated with risk of GA progression.[5,6,34] Irregular elevation of RPE/Bruch's membrane complex within the atrophic zone of GA as well as splitting of RPE/Bruch's membrane complex at two lesion borders has been associated with increased progression.[6] Recently, Folgar et al.[5] used semiautomated segmentation of the RPE/drusen complex in subjects from the AREDS2 ancillary SD-OCT study and found that abnormal thinning of the RPE/drusen complex was associated with new onset GA as well as development of central GA but did not specifically examine the impact on GA growth rate. Of note, Brar et al.[35] found that alterations in the RPE/Bruch's membrane complex at GA borders correspond to increased FAF, which suggests that there may be some redundancy in the predictive information provided by FAF and SD-OCT. The use of SD-OCT in identifying morphologic signatures of specific areas, which will progress to GA is a significant potential advantage when compared with FAF, which has not been shown to predict the location of GA lesion growth. However, additional studies are needed to realize this benefit. Fundus autofluorescence is advantageous in that it can be used to predict GA progression and is amenable to segmentation and quantification, even by nonexpert graders. Ultimately, multimodal imaging will likely provide the most robust predictive information. Thus, additional studies will be needed to determine, which combination of structural and functional imaging findings best predict the rate and location of GA lesion growth.

The current study has several limitations. One was reliance on a semiautomated software rather than a fully automated one to quantify GA. We note that a recent large prospective natural history study used semiautomated software[28] and that no such fully automated software has been tested on a large non–"cherry-picked" clinical dataset, which often suffer from a variety of distortions common in real-world clinical imaging. Thus, while our quantitative results are generated using semiautomated software, it is less subjective and time consuming than the previous studies based on manual image analysis. Additionally, the quantification of RAFH was fully automated, which removed subjectivity from the primary predictive component of the algorithm. Our study was also limited by relatively small size. However, GA progression rates in our study are similar to published values reported in other studies using FAF or color fundus photos to quantify GA suggesting that ours is a representative cohort. In our cohort, the median lesion size and rate of GA progression were 6.25 $mm^2$ and 1.68 $mm^2$/y, respectively. Previously, Holz et al.[10] reported a median lesion size of 7.04 $mm^2$ and median growth rate of 1.52 $mm^2$/y in 195 eyes and Bearelly et al.[25] reported a median growth rate of 1.49 $mm^2$/y in 45 eyes based on FAF imaging. Sunness et al.[36] reported a median growth rate of 2.1 $mm^2$/y in 212 eyes based on analysis of color fundus photos. Another limitation is that our study is retrospective and therefore demonstrates an association between RAFH and GA progression, but cannot prove that biology measured by RAFH is causative in GA progression. In the future, we plan a larger prospective multimodal imaging study to validate our algorithm and its findings and to compare predictions based on SD-OCT and FAF.

In conclusion, we have developed robust segmentation software that can be used to accurately predict risk of GA progression, and which makes predictions similar to validated but more cumbersome prediction algorithms. We also confirm and extend the previous finding that RAFH is correlated with rate of GA progression. Compared with other software available for GA quantification, ours has the advantage that it can be effectively used by nonexperts and requires minimal grader training. The use of semiautomated segmentation software allows rapid, accurate measurement of GA area and RAFH, and could aid both clinicians and researchers in predicting which patients will experience rapid progression in their GA. Future work will be focused on validating our software and the predictive value of RAFH in a larger, prospective observational study.

## Acknowledgments

The authors thank Sara Crowell for acting as clinical research coordinator for this study.

Disclosure: **M.J. Allingham**, None; **Q. Nie**, None; **E.M. Lad**, None; **D.J. Izatt**, None; **P.S. Mettu**, None; **S.W. Cousins**, None; **S. Farsiu**, None

## References

1. Klein R. Prevalence of age-related macular degeneration in the US population. *Arch Ophthalmol*. 2011;129:75.
2. Blair CJ. Geographic atrophy of the retinal pigment epithelium. A manifestation of senile macular degeneration. *Arch Ophthalmol*. 1975;93:19–25.
3. Giocanti-Auregan A, Tadayoni R, Fajnkuchen F, Dourmad P, Magazzeni S, Cohen SY. Predictive value of outer retina en face OCT imaging for geographic atrophy progression. *Invest Ophthalmol Vis Sci*. 2015;56:8325–8330.
4. Nunes RP, Gregori G, Yehoshua Z, et al. Predicting the progression of geographic atrophy in age-related macular degeneration with SD-OCT en face imaging of the outer retina. *Ophthalmic Surg Lasers Imaging Retina*. 44:344–359.
5. Folgar FA, Yuan EL, Sevilla MB, et al. Drusen volume and retinal pigment epithelium abnormal thinning volume predict 2-year progression of age-related macular degeneration. *Ophthalmology*. 2016;123:39–50, e1.
6. Moussa K, Lee JY, Stinnett SS, Jaffe GJ. Spectral domain optical coherence tomography-determined morphologic predictors of age-related macular degeneration-associated geographic atrophy progression. *Retina*. 2013;33:1590–1599.
7. Stetson PF, Yehoshua Z, Garcia Filho CAA, Portella Nunes R, Gregori G, Rosenfeld PJ. OCT minimum intensity as a predictor of geographic atrophy enlargement. *Invest Ophthalmol Vis Sci*. 2014;55:792–800.
8. Holz FG, Bellman C, Staudt S, Schütt F, Völcker HE. Fundus autofluorescence and development of geographic atrophy in age-related macular degeneration. *Invest Ophthalmol Vis Sci*. 2001;42:1051–1056.
9. Schmitz-Valckenberg S, Bindewald-Wittich A, Dolar-Szczasny J, et al. Correlation between the area of increased autofluorescence surrounding geographic atrophy and disease progression in patients with AMD. *Invest Ophthalmol Vis Sci*. 2006; 47:2648–2654.

10. Holz FG, Bindewald-Wittich A, Fleckenstein M, Dreyhaupt J, Scholl HPN, Schmitz-Valckenberg S. Progression of geographic atrophy and impact of fundus autofluorescence patterns in age-related macular degeneration. *Am J Ophthalmol*. 2007; 143:463–472.
11. Khanifar AA, Lederer DE, Ghodasra JH, et al. Comparison of color fundus photographs and fundus autofluorescence images in measuring geographic atrophy area. *Retina*. 2012; 32:1884–1891.
12. Schmitz-Valckenberg S, Brinkmann CK, Alten F, et al. Semi-automated image processing method for identification and quantification of geographic atrophy in age-related macular degeneration. *Invest Ophthalmol Vis Sci*. 2011;52:7640–7646.
13. Deckert A, Schmitz-Valckenberg S, Jorzik J, Bindewald A, Holz FG, Mansmann U. Automated analysis of digital fundus autofluorescence images of geographic atrophy in advanced age-related macular degeneration using confocal scanning laser ophthalmoscopy (cSLO). *BMC Ophthalmol*. 2005;5:8.
14. Delori FC, Dorey CK, Staurenghi G, Arend O, Goger DG, Weiter JJ. In vivo fluorescence of the ocular fundus exhibits retinal pigment epithelium lipofuscin characteristics. *Invest Ophthalmol Vis Sci*. 1995;36:718–729.
15. Sparrow JR, Wu Y, Nagasaki T, Yoon KD, Yamamoto K, Zhou J. Fundus autofluorescence and the bisretinoids of retina. *Photochem Photobiol Sci*. 2010;9:1480–1489.
16. Rudolf M, Vogt SD, Curcio CA, et al. Histologic basis of variations in retinal pigment epithelium autofluorescence in eyes with geographic atrophy. *Ophthalmology*. 2013;120:821–828.
17. Sparrow JR, Boulton M. RPE lipofuscin and its role in retinal pathobiology. *Exp Eye Res*. 2005;80:595–606.
18. Lois N, Owens SL, Coco R, Hopkins J, Fitzke FW, Bird AC. Fundus autofluorescence in patients with age-related macular degeneration and high risk of visual loss. *Am J Ophthalmol*. 2002;133:341–349.
19. Einbock W, Moessner A, Schnurrbusch UEK, Holz FG, Wolf S. Changes in fundus autofluorescence in patients with age-related maculopathy. Correlation to visual function: a prospective study. *Graefes Arch Clin Exp Ophthalmol*. 2005;243: 300–305.
20. Hwang JC, Chan JWK, Chang S, Smith RT. Predictive value of fundus autofluorescence for development of geographic atrophy in age-related macular degeneration. *Invest Ophthalmol Vis Sci*. 2006;47:2655–2661.
21. Bindewald A, Schmitz-Valckenberg S, Jorzik JJ, et al. Classification of abnormal fundus autofluorescence patterns in the junctional zone of geographic atrophy in patients with age related macular degeneration. *Br J Ophthalmol*. 2005;89:874–878.
22. Fleckenstein M, Schmitz-Valckenberg S, Lindner M, et al. The "diffuse-trickling" fundus autofluorescence phenotype in geographic atrophy. *Invest Ophthalmol Vis Sci*. 2014;55: 2911–2920.
23. Jeong YJ, Hong IH, Chung JK, Kim KL, Kim HK, Park SP. Predictors for the progression of geographic atrophy in patients with age-related macular degeneration: fundus autofluorescence study with modified fundus camera. *Eye*. 2014;28:209–218.
24. Biarnés M, Monés J, Trindade F, Alonso J, Arias L. Intra and interobserver agreement in the classification of fundus autofluorescence patterns in geographic atrophy secondary to age-related macular degeneration. *Graefes Arch Clin Exp Ophthalmol*. 2012;250:485–490.
25. Bearelly S, Khanifar AA, Lederer DE, et al. Use of fundus autofluorescence images to predict geographic atrophy progression. *Retina*. 2011;31:81–86.
26. Estrada R, Tomasi C, Cabrera MT, Wallace DK, Freedman SF, Farsiu S. Exploratory Dijkstra forest based automatic vessel segmentation: applications in video indirect ophthalmoscopy (VIO). *Biomed Opt Express*. 2012;3:327–339.
27. Lindner M, Böker A, Mauschitz MM, et al. Directional kinetics of geographic atrophy progression in age-related macular degeneration with foveal sparing. *Ophthalmology*. 2015;122: 1356–1365.
28. Schmitz-Valckenberg S, Sahel J-A, Danis R, et al. Natural history of geographic atrophy progression secondary to age-related macular degeneration (Geographic Atrophy Progression Study). *Ophthalmology*. 2016;123:361–368.
29. Yehoshua Z, Rosenfeld PJ, Gregori G, et al. Progression of geographic atrophy in age-related macular degeneration imaged with spectral domain optical coherence tomography. *Ophthalmology*. 2011;118:679–686.
30. Marsiglia M, Boddu S, Bearelly S, et al. Association between geographic atrophy progression and reticular pseudodrusen in eyes with dry age-related macular degeneration. *Invest Ophthalmol Vis Sci*. 2013;54:7362–7369.
31. Zweifel SA, Engelbert M, Laud K, Margolis R, Spaide RF, Freund KB. Outer retinal tubulation: a novel optical coherence tomography finding. *Arch Ophthalmol*. 2009;127:1596–1602.
32. Hariri A, Nittala MG, Sadda SR. Outer retinal tubulation as a predictor of the enlargement amount of geographic atrophy in age-related macular degeneration. *Ophthalmology*. 2015;122: 407–413.
33. Bearelly S, Chau FY, Koreishi A, Stinnett SS, Izatt JA, Toth CA. Spectral domain optical coherence tomography imaging of geographic atrophy margins. *Ophthalmology*. 2009;116:1762–1769.
34. Leuschen JN, Schuman SG, Winter KP, et al. Spectral-domain optical coherence tomography characteristics of intermediate age-related macular degeneration. *Ophthalmology*. 2013;120: 140–150.
35. Brar M, Kozak I, Cheng L, et al. Correlation between spectral-domain optical coherence tomography and fundus autofluorescence at the margins of geographic atrophy. *Am J Ophthalmol*. 2009;148:439–444.
36. Sunness JS, Margalit E, Srikumaran D, et al. The long-term natural history of geographic atrophy from age-related macular degeneration: enlargement of atrophy and implications for interventional clinical trials. *Ophthalmology*. 2007;114:271–277.